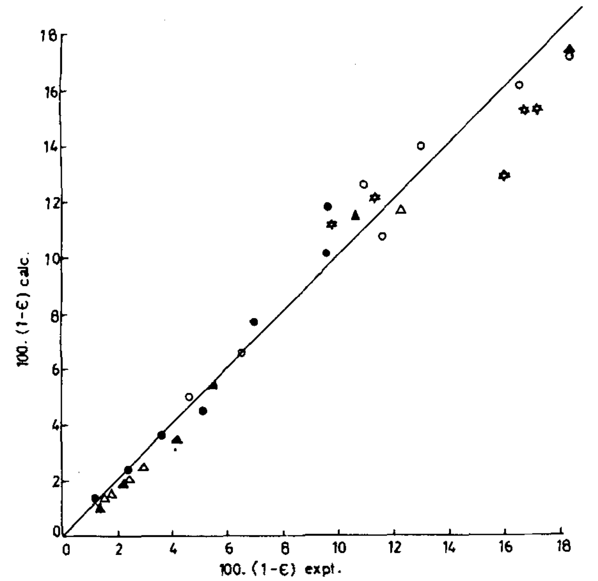

Figure 2. Comparison of experimental and predicted *in-situ* solid concentration. For legend, see Table 1.

can differ substantially which is due to the inherent slip existing between the solid and the fluid. The value of v_s/v_f varied between 0.6 and 1 in the present experiments. In any pressure drop correlation this fact has to be incorporated.

The *in-situ* solid concentration can be obtained from Eqs. 12 and 17. It must be emphasized, however, that the range of experimental conditions on which Eq. 17 is based is not very wide. However, till a comprehensive relation valid over a wide range of operating conditions is developed, Eqs. 12 and 17 can serve as useful first approximations in the design of hydraulic transportation systems.

NOTATION

a = ratio of solid to fluid velocity, dimensionless
A = area of cross section of the pipe, cm^2
b = the ratio n/ϵ_d, dimensionless
d_p = particle diameter, cm
D = pipe diameter, cm
Fr = $v_m/\sqrt{gD}$, dimensionless
g = acceleration due to gravity, cm/s^2
Ga = $d_p^3 g\rho(\rho_p - \rho)/\mu^2$, dimensionless
n = exponent in Eq. 7, dimensionless
N = defined in Eq. 15, dimensionless
Q = volumetric slurry flow rate, equals $(Q_s + Q_f)$, cm^3/s
Q_f = volumetric fluid flow rate, cm^3/s
Q_s = volumetric solid flow rate, cm^3/s
Re = $d_p u_t \rho/\mu$, dimensionless
u_t = terminal settling velocity of particle, cm/s
v_f = actual fluid velocity inside the pipe, cm/s
v_s = actual solid velocity inside the pipe, cm/s
v_m = mixture velocity, Q/A, cm/s

Greek Letters

ϵ = *in-situ* fluid voidage or porosity, dimensionless
ϵ_d = delivered fluid voidage or porosity, dimensionless
μ = fluid viscosity, g/(cm·s)
ρ = fluid density, g/cm^3
ρ_p = particle density, g/cm^3
$(1 - \epsilon)$ = *in-situ* concentration of solids, dimensionless
$(1 - \epsilon_d)$ = delivered concentration of solids, dimensionless

LITERATURE CITED

Gandhi, R. L., "An Analysis of Hold-Up Phenomena in Slurry Pipelines," *Hydrotransport 4*, BHRA, A3-33 (1976).

Kao, D. T., A. Nosrati, and J. L. Schaefer, "Flow Behaviour of Solid-Liquid Mixtures in Pipes on Positive and Negative Grades," *Hydrotransort 7*, BHRA, F1-215 (1980).

Spedding, P. L., and V. T. Nguyen, "Hold-Up in Fluid-Solid Two-Phase Flow," *Chem. Eng. J.*, **15**, p. 131 (1978).

Televentos, Y., C. Shook, A. Carleton, and M. Streat, "Flow of Slurries of Coarse Particles at High Solids Concentrations," *Can. J. Chem. Eng.*, **57**, p. 255 (1979).

Wani, G. A., "Hydraulic Transportation of Solids Through Horizontal Pipes," Ph.D. Thesis, Indian Institute of Technology, Delhi (1982).

ACKNOWLEDGMENT

The experiments reported here were performed by G. A. Wani.

Manuscript received October 5, and accepted December 17, 1982.

Extension of Nichols Chart for Identification of Open-Loop Unstable Systems

S. P. SRINIVAS,
P. B. DESHPANDE, and
P. R. KRISHNASWAMY

Department of Chemical Engineering
University of Louisville
Louisville, KY 40292

Recently Deshpande (1980) described a technique for dynamic identification of open-loop unstable systems. His method involves first obtaining experimental values for the closed-loop magnitude ratio, M, and phase angle, α, by pulse or step test implemented on a system stabilized with an arbitrarily tuned feedback controller. The corresponding open-loop magnitude ratio, A, and phase lag, θ (which exhibit unstable characteristics) are then obtained from Nichols chart via back calculation. The back calculation procedure is essentially the reverse of normal chart reading, i.e., fixing numerous closed-loop data points on the Nichols chart by manual

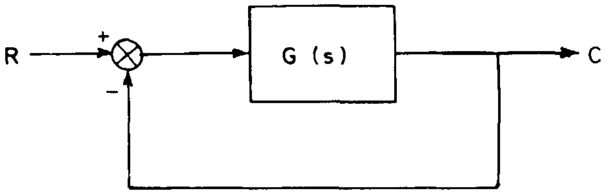

Figure 1. Basic unity feedback control loop.

interpolation of the M and α contours and reading off the corresponding open-loop (A and θ) values as projections on the x and y axes.

The purpose of this paper is to show that no back calculation need be adopted for this purpose and that the open-loop unstable response can be obtained in an explicit and easy manner by employing the normal straightforward Nichols chart procedure. In other words, apart from the well-known concept that the Nichols chart is made up of constant M and α contours plotted against A and θ for deriving the closed-loop frequency response, it will be shown here that the same chart serves also as a network of A and θ contours plotted against M and α axes for the purpose of unstable open-loop identification. The fundamental relationship which permits this dual interpretation to Nichols chart will be established here.

Consider a unity feedback control system shown in Figure 1. The open-loop transfer function, $G(s)$, represents an unstable process, several examples of which are available (Koppel, 1966; Luyben, 1972, 1974; Luyben and Melcic, 1978; Deshpande, 1980). $G(s)$ also typically includes a controller and a final control element. The problem is to identify $G(s)$ assuming that the frequency response version of the corresponding stable closed-loop transfer function, $G^*(s)$, is available.

From Figure 1, $G^*(s)$, is given as

$$G^*(s) = \frac{C}{R} = \frac{G(s)}{1 + G(s)} \tag{1}$$

Equation 1 may be rewritten as

$$G(s) = \frac{G^*(s)}{1 - G^*(s)} \tag{2}$$

Let $G(jw) = A\angle\theta = A \cos\theta + jA \sin\theta$ (3a)

and $G^*(jw) = M\angle\alpha = M \cos\alpha + jM \sin\alpha$ (3b)

It can be shown (Coughanowr and Koppel, 1965) from Eqs. 1 and 3a that

$$M = \frac{A}{\sqrt{1 + 2A \cos\theta + A^2}} \tag{4a}$$

and

$$\alpha = \tan^{-1}\left(\frac{\sin\theta}{\cos\theta + A}\right) \tag{4b}$$

Similarly it can be shown from Eqs. 2 and 3b that

$$A = \frac{M}{\sqrt{1 - 2M \cos\alpha + M^2}} \tag{5a}$$

and

$$\theta = \tan^{-1}\left(\frac{\sin\alpha}{\cos\alpha - M}\right) \tag{5b}$$

Equations 5a and 5b have the same form as Eqs. 4a and 4b suggesting that the inverse Nichols chart (lines of constant A and θ on coordinates of M and α) must have a similar profile as the normal one. A close observation further reveals that the conventional Nichols chart itself can be used for the reverse process of open-loop identification. The generalization to be effected for this purpose can be explicitly seen by imposing the condition

$$A = M \tag{6}$$

in Eqs. 4a and 5a. Then, from Eqs. 4a and 6, we get

$$M = -2 \cos\theta \tag{7}$$

and from Eqs. 5a and 6,

$$A = 2 \cos\alpha \tag{8}$$

The last three equations yield

$$\cos\theta + \cos\alpha = 0 \tag{9}$$

for which the solutions are

$$\theta = \pi + \alpha \tag{10a}$$

$$\theta = -\pi + \alpha \tag{10b}$$

$$\theta = -\pi - \alpha \tag{10c}$$

$$\theta = \pi - \alpha \tag{10d}$$

Of these the only two distinct solutions are Eqs. 10a and 10b. The remaining solutions are trivially the same and hence can be ignored. Further, without loss of generality we may assume that Eq. 10a

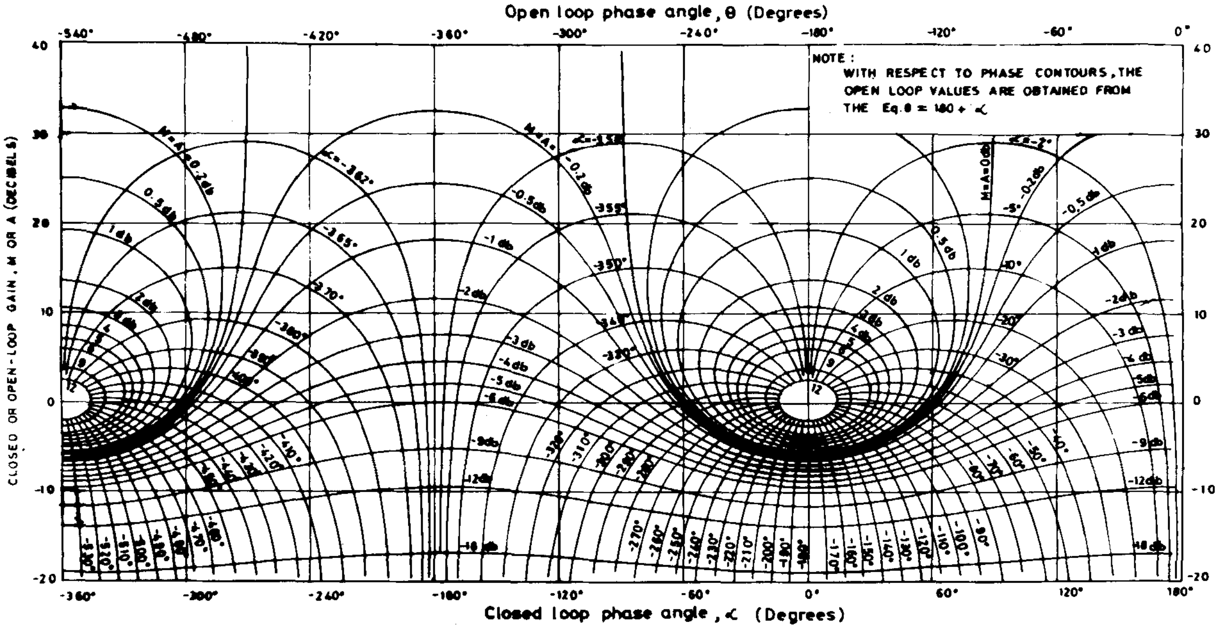

Figure 2. Generalized Nichols chart.

corresponds to the phase contours and Eq. 10b to the x-axis so that the resulting plot conforms to the conventional Nichols chart. Figure 2 illustrates this from where it can be seen that incorporation of Eqs. 6, 10a, and 10b as above into the Nichols chart makes it so generalized and versatile as to permit both open- and closed-loop process identification. Thus, in addition to the usual M and α contours plotted on the A and θ coordinates, Figure 2 also provides loci of constant A and θ superimposed on the M and α coordinates. It may be noted from the chart that, while the M and A values coincide, the α and θ values differ from each other by a constant factor of 180° as per Eqs. 10a and 10b. Using Figure 2 the closed-loop (or open-loop) identification is achieved by the usual procedure of entering the chart through A and θ (or M and α) coordinates, and reading of M and α (or A and θ) contour values by interpolation. Any existing computer program describing the conventional Nichols chart may also be used for open-loop identification simply by incorporating Eqs. 6, 10a and 10b into the program.

NOTATION

A = open-loop magnitude ratio
C = controlled variable
$G(s)$ = open-loop process transfer function
$G^*(s)$ = closed-loop process transfer function
j = $\sqrt{-1}$
M = closed-loop magnitude ratio
R = set point
w = frequency, radians/time

Greek Letters

α = closed-loop phase angle, degrees
θ = open-loop phase angle, degrees

LITERATURE CITED

Coughanowr, D. R., and L. B. Koppel, *Process Systems Analysis and Control*, McGraw Hill, New York (1965).

Deshpande, P. B., "Process Identification of Open-loop Unstable Systems," *AIChE J.*, **26**, p. 305 (1980).

Koppel, L. B., "Sampled Data Control of Unstable Processes," *Ind. Eng. Chem. Fund.*, **5**, p. 396 (1966).

Luyben, W. L., "Sample-Data Control of Second-Order Open-loop Unstable Processes," *Ind. Eng. Chem. Fund.*, **1**, p. 557 (1972).

Luyben, W. L., "Effect of Reaction Rate on the Open-Loop Stability of Chemical Reactors," AICHE J., 26, p. 175 (1974).

Luyben, W. L., and M. Melcic, "Consider Reactor Control Lags," *Hydroc. Proc.*, **6**, p. 115 (1978).

Manuscript received February 23, and accepted December 17, 1982.

Accelerated Convergence for Newton-Type Iterations Applied to Multicomponent Distillation Problems

D. S. BILLINGSLEY

IBM Corp.
Two Riverway
Houston, TX 77056

INTRODUCTION

The component material balances and equilibrium relations on all the stages in a distillation column at steady state may be expressed in the well known form of a matrix-vector equation

$$A_i \Upsilon_i = f_i, \quad i = 1, \ldots, I \tag{1}$$

where A_i is a tridiagonal matrix involving equilibrium ratios, K_{ij}, of component i and ratios, L_j/V_{j+1}, of phase flow rates, but having no explicit dependence upon mole fractions. Υ_i is a vector of vapor flow rates of component i on all stages. f_i is a vector of molar feed rates of component i on all stages. Thus the elements of f_i are zero except for elements corresponding to feed stages.

Two computational procedures, successive approximation and simultaneous solution, are currently usually used for solving multicomponent staged distillation problems. The solution of Eq. 1 plays a central role in each approach. The scheme of Boston and Sullivan (1972) is probably the most efficient available for solving Eq. 1. This algorithm is the only one able to produce a solution while employing only multiplication and addition of positive numbers.

The successive approximation computational procedure consists of solving Eq. 1, correcting that solution, determining new estimates of stage temperatures as the bubble points of the corrected mole fractions, and using these temperatures in the heat balances to compute new estimates of phase flows. Various methods are used to correct the solution to Eq. 1. Holland (1963) multiplies all the product ratios, d_i/b_i, by a single correction factor, θ, and determines θ so that a product specification is satisfied. Boston and Sullivan (1974) in effect multiply all the ratios L_j/V_{j+1} by a single correction factor, S, and then determine S so that a product specification is satisfied. Alternately one could assume that all stage temperatures were multiplied by a constant factor or incremented by a constant addend. In any case the equation for determining the correction factor is nonlinear and usually solved by Newton iterations. Analytic partial derivatives with respect to the correction factor are simple to evaluate. For instance, partials with respect to S are readily obtained by differentiating Eq. 1.

As considered here the simultaneous solution computational procedure is based upon linearization of all equations under the assumptions that equilibrium ratios are independent of composition and that phase enthalpies may have an explicit linear composition dependence (Gentry, 1970; Billingsley and Boynton, 1971). A distinguishing feature of this procedure is that neither component flow rates nor mole fractions are "iteration variables." In effect, one formally solves Eq. 1, sums these solutions to have

$$(V_{J+1}, \ldots, V_1)^T = \sum_i \Upsilon_i = \sum_i A_i^{-1} f_i \tag{2}$$

and also substitutes the solutions of Eq. 1 into the heat balances. The result is a set of equations in which the only unknowns are the stage temperatures and the vapor phase flows. Note that vapor-phase